

## ORIGINAL ARTICLE

# THC Exposure is Reflected in the Microstructure of the Cerebral Cortex and Amygdala of Young Adults

Ryan P. Cabeen<sup>1</sup>, John M. Allman<sup>2</sup> and Arthur W. Toga<sup>1</sup>

<sup>1</sup>Laboratory of Neuro Imaging, USC Stevens Neuroimaging and Informatics Institute, Keck School of Medicine of USC, University of Southern California, Los Angeles, CA 90033, USA and <sup>2</sup>Division of Biology, California Institute of Technology, Pasadena, CA 91125, USA

Address correspondence to Ryan P. Cabeen, Laboratory of Neuro Imaging, USC Stevens Neuroimaging and Informatics Institute, Keck School of Medicine of USC, University of Southern California, Los Angeles, CA 90033, USA. Email: rcabeen@loni.usc.edu.

## Abstract

The endocannabinoid system serves a critical role in homeostatic regulation through its influence on processes underlying appetite, pain, reward, and stress, and cannabis has long been used for the related modulatory effects it provides through tetrahydrocannabinol (THC). We investigated how THC exposure relates to tissue microstructure of the cerebral cortex and subcortical nuclei using computational modeling of diffusion magnetic resonance imaging data in a large cohort of young adults from the Human Connectome Project. We report strong associations between biospecimen-defined THC exposure and microstructure parameters in discrete gray matter brain areas, including frontoinsular cortex, ventromedial prefrontal cortex, and the lateral amygdala subfields, with independent effects in behavioral measures of memory performance, negative intrusive thinking, and paternal substance abuse. These results shed new light on the relationship between THC exposure and microstructure variation in brain areas related to salience processing, emotion regulation, and decision making. The absence of effects in some other cannabinoid-receptor-rich brain areas prompts the consideration of cellular and molecular mechanisms that we discuss. Further studies are needed to characterize the nature of these effects across the lifespan and to investigate the mechanistic neurobiological factors connecting THC exposure and microstructural parameters.

**Key words:** Amygdala, cerebral cortex, diffusion MRI, microstructure, tetrahydrocannabinol (THC)

## Introduction

The endocannabinoid system is known to serve a critical homeostatic role in the central nervous system (Volkow et al., 2017; Silvestri and Di Marzo, 2013), in which it modulates appetite, pain, stress, and reward processing (Tarragon and Moreno, 2017; Freund et al., 2003; Mackie and Stella, 2006); yet, there remain open questions regarding its relation to behavior and response to exogenous cannabinoids. Molecular biological studies have shown that it functions through retrograde signaling of cannabinoid neurotransmitters (Kreitzer and Regehr, 2002; Hua et al., 2016; Devane et al., 1992) that modulate cellular function by binding endocannabinoid receptors (Hua et al., 2016; Devane et al., 1992), which are found throughout the brains of mammals with varied density based on cell type and brain area

(Herkenham et al., 1990; Devane et al., 1988; Glass et al., 1997). Cannabis is a plant whose consumption produces modulatory effects on the endocannabinoid system, making it a fixture of human societies spanning an array of uses and contexts (National Academies of Sciences, Engineering, and Medicine and others, 2017; Long et al., 2017; Grotenhermen, 2003). In particular, it produces psychotropic effects such as euphoria and relaxation that are considered driving factors in recreational usage (Green et al., 2003; van Hell et al., 2011). Until recently, there have been restricted avenues for legal cannabis use and research, but regulatory changes have expanded what cannabis products are available, the ways in which the public consumes them, and the possibilities for research (Haney and Hill, 2018; Hasin, 2017). This presents a need for better understanding the specific ways

that cannabis affects the brain and the consequent changes in behavior (Murray et al., 2007; Hall and Degenhardt, 2009).

Epidemiological and pharmacological studies have shed light on the effects of cannabis, indicating both therapeutic applications and health risks associated with its use (National Academies of Sciences, Engineering, and Medicine and others, 2017; Hall, 2015; Volkow et al., 2014). While cannabis has many neuropharmacologically active agents, tetrahydrocannabinol (THC) is the primary psychoactive compound that motivates its recreational usage (Andre et al., 2016; ElSohly et al., 2014). It acts as a partial agonist on type 1 cannabinoid receptor (CB1) (Grotenhermen, 2003), in which it modulates the function of the endocannabinoid system to alter mood, perception and appetite and produce a characteristic relaxed or euphoric state (Agrawal et al., 2014; Mattes et al., 1994) with acute side effects including reduced short-term memory, impaired motor skills, and heightened anxiety and paranoia (Gonzalez, 2007). Studies of long-term neurological effects of THC exposure have shown reversible downregulation of CB1 receptors (Hirvonen et al., 2012), impaired cognition (Broyd et al., 2016; Batalla et al., 2013), and increased risk of psychosis, particularly in adolescence (Marconi et al., 2016; Large et al., 2011; Moore et al., 2007; Andrade, 2016). In contrast, studies of therapeutic applications of THC have found substantial support for its use in treating chronic pain (Smith et al., 2015; Andrae et al., 2015) and chemo-therapy induced nausea and vomiting (Grotenhermen and Müller-Vahl, 2012; Whiting et al., 2015; Smith et al., 2015).

Magnetic resonance imaging (MRI) has emerged as a useful tool for delineating the structural and functional changes associated with THC exposure, and these findings have been comprehensively reviewed (Bloomfield et al., 2018; Lisdahl et al., 2014; Batalla et al., 2013; Quickfall and Crockford, 2006). Cerebral blood flow (CBF) imaging studies have identified changes in prefrontal and insular areas (Mathew et al., 1997; van Hell et al., 2011), and functional MRI studies have expanded this picture to identify network-level and task-dependent changes in brain connectivity during THC exposure. Several studies have shown disruptions in salience processing, i.e., changes in connectivity of insular and anterior cingulate regions with other brain areas (Bhattacharyya et al., 2015; Wetherill et al., 2015; Battistella et al., 2013; Hester et al., 2009; Bhattacharyya et al., 2012). There is further evidence of functional alterations of fear and emotion processing in areas such as the amygdala (Phan et al., 2008; Colizzi et al., 2018; Heitzeg et al., 2015), and task-specific findings showing effects related to motor inhibition (Borgwardt et al., 2009), reward anticipation (Nestor et al., 2010), spatial working memory (Schweinsburg et al., 2010), and cognitive control (Harding et al., 2012). In contrast, structural neuroimaging has provided a complementary picture of associations of THC exposure with brain morphology and tissue properties of gray and white matter. Morphometric studies have found effects in subcortical gray matter structures, such as the nucleus accumbens, amygdala, and hippocampus (Lorenzetti et al., 2019; Gilman et al., 2014; Owens et al., 2019), as well as cortical effects in gray matter density in prefrontal areas, insular cortex, and the cerebellum (Medina et al., 2010; Churchwell et al., 2010; Battistella et al., 2014). Similar to functional studies, gray matter effects have been detected that are specifically related to psychosis (Schnell et al., 2012). More refined analysis has further shown cortical thinning in prefrontal and insular cortex (Lopez-Larson et al., 2011; Jacobus et al., 2015; Shollenbarger et al., 2015). Diffusion imaging has revealed white matter effects (Becker et al., 2015; Yücel et al., 2010; Jacobus et al., 2013; Orr et al., 2016), with

consistent results in the corpus callosum (Arnone et al., 2008; Zalesky et al., 2012; Rigucci et al., 2015), in adolescence (Ashtari et al., 2009), and in relation to impulsivity (Gruber et al., 2011). Together, these imaging studies provide substantial support for numerous and persistent changes in the brain function and structure related to THC exposure; however, there remain open questions regarding the neuroanatomical features related to tissue organization that are involved.

In this study, we investigated how microstructure organization relates to THC exposure, focusing on the cerebral cortex, and subcortical nuclei involved in decision making and emotion regulation. While gray matter morphology and volumetry approaches are powerful tools, they provide measures of neuroanatomy that are relatively coarse-grain and non-specific to the underlying tissue organization. Our experiments use recent advances in multi-shell diffusion MRI and computational modeling techniques to probe aspects of the organizational properties of tissue microstructure that have been previously unexplored in relation to THC exposure. Our analysis is distinguished from past diffusion MRI studies of THC exposure that focused on white matter tissue properties; in contrast, we examined gray matter imaging parameters, which may capture distinct microstructural features of neurites and glial cells. Our experiments specifically characterized the relationship between gray matter microstructure imaging parameters and biospecimen-defined THC exposure in a large cohort of typical young adults recruited and scanned cross-sectionally as part of the Human Connectome Project (HCP), using a multi-modal and computational approach to derive quantitative indices of tissue microstructure. Our analysis primarily examined fronto-insular cortex and subcortical brain areas (nucleus accumbens, caudate, putamen, substantia nigra, hippocampus, hypothalamus, and periaqueductal gray), and in a subsequent analysis, we expanded the analysis across the cerebral cortex to assess the anatomical specificity of our results. We report differences in an index of neurite orientation dispersion (ODI) that are localized in bilateral fronto-insular and ventromedial prefrontal cortex and the lateral subfields of the amygdala, with analogous findings shown with fractional anisotropy (FA) using diffusion tensor imaging (DTI). Our analysis further investigated the connection between these findings and individual behavioral measures, showing independent effects in memory performance, negative intrusive thinking, and paternal substance abuse. We discuss the relevance of these findings and the connection of THC exposure with brain areas underlying salience processing, emotion regulation, and decision making. We did not detect microstructural effects in all cannabinoid-receptor-rich brain areas, which motivates several hypotheses concerning redundant molecular and cellular mechanisms that we propose to potentially explain our findings.

## Materials and Methods

### Participants and Datasets

Data were acquired from participants as part of the HCP. We obtained T<sub>1</sub>-weighted (T1wMRI) and diffusion-weighted MRI (dwMRI) data, and included 781 participants with scans that pass quality control and completed image processing. Following institutional ethics review, we also analyzed demographic and behavioral data from the restricted data release, which included age, gender, self-reported substance use, and self-reported family history of substance abuse. Biospecimen-defined THC exposure was assessed with a urine screen

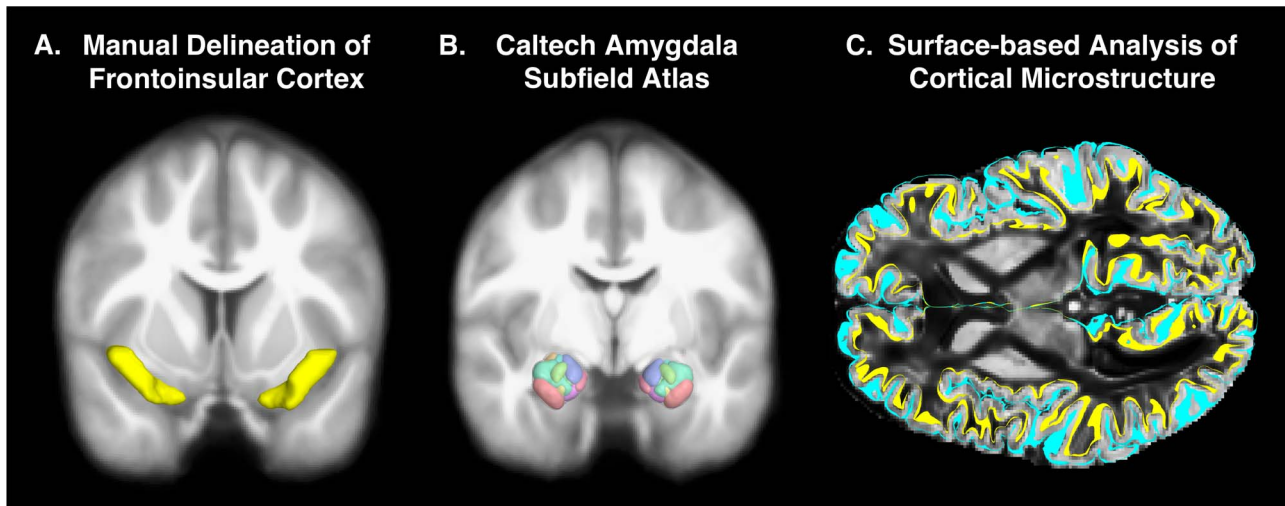


**Figure 1.** An overview of the anatomical modeling components used in our analysis. (A) shows the manually drawn frontoinsular cortex mask used in the region of interest analysis, and (B) shows amygdala subfields that were obtained from the Caltech Amygdala Atlas and included as well (T1wMRI shown in background). (C) illustrates the cortical surface analysis, in which the pial boundary (cyan) and white matter boundary (yellow) were used to estimate cortical microstructure (ODI shown in background) in brain areas from the HCP multimodal parcellation.

(Alere iScreen 6-panel urine drug test dip card; DOA164–551), and 85 participants were included that tested positive for THC exposure, as determined as per the manufacturer’s criterion cut-off of 50 ng/mL of the THC metabolite 11-nor- $\Delta^9$ -tetrahydrocannabinol-9-carboxylic acid (THCCOOH). We also examined an additional self-reported total number of cannabis uses, which consisted of the the following levels: no use=0; 1–5 uses=1; 6–10 uses=2; 11–101 uses=3; 101–999 uses=4; 1000 or more uses=5. Participants completed a set of instruments from the Achenbach System of Empirically Based Assessment (ASEBA) (Achenbach and Rescorla, 2003), and from this, we retained the adult self-report thought problems scale (Abdellaoui et al., 2012). We used this scale to operationalize a summary measure of negative intrusive thinking, as the questionnaire includes self-reported measures of hallucinations, self-destructive thoughts, repetitive behavior and other factors that negatively impact daily life. Working memory was assessed using the NIH Toolbox, and our analysis examined the overall accuracy across all conditions.

### Image Acquisition and Preprocessing

T1wMRI and dwMRI data from the HCP were collected on a Connectome Siemens 3 Tesla Skyra scanner using a 32-channel head coil (Glasser et al., 2013; Van Essen et al., 2013). The T1wMRIs were acquired using a 3D MPRAGE sequence with 0.7 mm isotropic resolution (FOV=224 mm, matrix=320, 256 sagittal slices in a single slab), repetition time (TR)=2400 ms, echo time (TE)=2.14 ms, inversion time (TI)=1000 ms, flip angle=8°, bandwidth=210 Hz per pixel, echo spacing=7.6 ms, and phase encoding undersampling factor GRAPPA=2.10%. dwMRIs were collected with a single-shot two dimensional spin-echo EPI acquisition with a multi-band factor of 3, 1.25 mm isotropic voxels with FOV PE by Readout=210×180; matrix size PE by Readout=144×168; 111 interleaved slices without gap; left–right and right–left phase encoding; flip angles=78° and 160°. For each phase encoding direction, the diffusion sampling scheme consisted of 18 baseline scans and 270 diffusion-weighted scans acquired using single diffusion encoding across

3 shells with  $b=1000, 2000,$  and  $3000$  s/mm<sup>2</sup>; all dwMRI scans had TE=89 ms and TR=5.5 s. Each shell included 192 data points representing 90 diffusion gradient directions and 6  $b=0$  shells acquired twice resulting in 270 non-collinear directions for each PE. Total acquisition time was approximately 54 min (6 segments of 9 min each). dwMRI data were preprocessed with the HCP workflow (Sotiropoulos et al., 2013). This included a sophisticated approach for correction of artifact due to motion and eddy-current and susceptibility induced geometric distortion. Using an additional set of diffusion MRI scans collected with reversed phase encoding, this scheme estimates and corrects for the off-resonance field and subject head motion using a Gaussian process framework for robust non-parametric interpolation of the dwMRI signal.

### Image Analysis

The HCP data were subsequently analyzed using the LONI Pipeline (Dinov et al., 2009) to obtain microstructure parameters characterizing the cerebral cortex and subcortical nuclei. The workflow was implemented with the Quantitative Imaging Toolkit (QIT) (Cabeen et al., 2018), Freesurfer (Fischl, 2012), FSL (Jenkinson et al., 2012), ANTs (Avants et al., 2008), and DTI-TK (Zhang et al., 2006). The main components are illustrated in Figure 1 and described as follows.

The dwMRI data were denoised using a non-local means filter, and microstructure parameters were obtained using two multi-shell modeling approaches. First, we performed neurite orientation dispersion and density imaging (NODDI) (Zhang et al., 2012) and estimated its parameters using a non-linear fitting approach accelerated using the spherical mean technique (Cabeen et al., 2019), resulting in volumetric maps of the orientation dispersion index (ODI), neurite density index (NDI) and isotropic volume fraction (ISO). Because our experiments look specifically at gray matter, we used a parallel diffusivity of  $1.1 \times 10^{-3}$  mm<sup>2</sup>/s, which is an optimized value obtained from previous work (Fukutomi et al., 2018). NDI is meant to depict the proportion of neurite volume relative to the total

cellular volume, while ODI is meant to separately depict neurite orientational heterogeneity. We also estimated DTI (Basser and Jones, 2002) parameters using weighted linear least squares fitting with free-water elimination with a fixed diffusivity of  $3.0 \times 10^{-3}$  mm<sup>2</sup>/s in the isotropic compartment (Hoy et al., 2014), resulting in volumetric maps of FA and mean diffusivity (MD). We then created a population-averaged dataset from 88 scans from the test-retest portion of the HCP dataset. We used the tensor-based deformable registration and spatial normalization pipeline implemented in DTI-TK (Zhang et al., 2007) to produce the population averaged DTI, NODDI, and T1wMRI datasets that were aligned to the IIT template (Zhang et al., 2011). Subject data from all participants were then spatially normalized to the template and the deformable registration maps were retained for each individual.

Our initial goal was to investigate gray matter microstructure parameters in fronto-insular cortex (FIC) and related structures involved with decision making and emotion regulation using a region-of-interest (ROI) approach. We subsequently expanded our analysis to include cannabinoid-receptor-rich brain areas. Guided by the definition from Allman et al. (2010), we first manually delineated ROIs on coronal slices of the template for left and right FIC using QIT and co-registered these in subject native space and computed region-averaged parameters. The other additional structures we examined included: the nucleus accumbens, caudate, putamen, substantia nigra (separate compact and reticular parts), hippocampus, hypothalamus and periaqueductal gray. ROIs were obtained from the Caltech Subcortical and Amygdala Atlases (Pauli et al., 2018; Tyszka and Pauli, 2016), and the remainder were manually drawn on the population average. The Caltech atlas data were aligned to our population average T1wMRI map using ANTs diffeomorphic registration, and the amygdala atlas includes 10 subfields that are described in detail in the publication associated with the atlas.

In a subsequent analysis, we also investigated microstructure properties across the entire cerebral cortex, with the goal of determining the anatomical specificity of the fronto-insular findings in the ROI analysis. We processed T1wMRI data using Freesurfer to create 3D cortical models, and the cortical models were linearly aligned with the diffusion data using FSL FLIRT with the mutual information cost function. To estimate cortical microstructure, we took a similar approach to Fukutomi et al. (2018) and refined the alignment of the cortical surface to better match the tissue boundaries in the diffusion scan, which may retain subtle geometric distortions not found in the T1wMRI. Briefly, for each subject, we computed the weighted average microstructure parameters in each vertex of the Freesurfer cortical surface, which was aligned to native diffusion space. The surface-based parameter average was computed in two stages. In the first stage, the midpoint between the pial and white matter surfaces was computed and 15 sampling points were equally spaced between them, with an additional 2 mm buffer on either side. For a given microstructure parameter, the values were measured at each of the sampling points, and subsequently inversely weighted by their distance to the midpoint and the by tissue MD, with the goal of avoiding contamination by white matter and CSF. In the second stage, the mean and standard deviation were computed and outlier values were detected and excluded using a z-score threshold of 3.0; finally, the average value was found from the remaining points. We then summarized the microstructure parameters in the regions defined by the HCP multi-modal parcellation (HCP-MMP-

1.0), which includes 180 cytoarchitecturally defined parcels in each hemisphere (Glasser et al., 2016). The HCP-MMP-1.0 region most closely aligned with the manually drawn fronto-insular ROI was agranular anterior insular cortex (AAIC). For each subject, we also created a composite ventro-medial prefrontal cortex (vmPFC) region by averaging the microstructure parameters from Brodmann areas p32, s32, a24, and 10r, and we computed interhemispheric averages of the AAIC and vmPFC measures as well.

## Statistical Analysis

We first estimated multiple linear regression models to relate microstructure to the subject variables with covariates including: age, gender, body mass index (BMI), intracranial volume, and whether the subject was a daily smoker or drinker. All continuous model parameters were normalized to zero-mean and unit-variance to allow their regression coefficients to be reported in standardized units. We excluded outliers using Tukey's procedure, in which high and low cutoffs were determined by 1.5 times the interquartile range beyond the low and high quartiles, computed using the entire cohort. Covariates were added using forward stepwise model selection; after which, the variable-of-interest, e.g., THC exposure, was included in the model. We used the Bayesian Information Criteria (BIC) for model selection, a statistical measure that balances model complexity and goodness-of-fit (Vrieze, 2012). We retained the  $R^2$  coefficient of determination of the model, and the statistical outcomes of each subject variable, including the regression coefficient, *t*-value, standard error, and *P*-value. To measure the support for including THC exposure in models explaining microstructure variation, we also retained the change in adjusted  $R^2$  and change in BIC between models with and without THC exposure. For data from the surface-based analysis with the HCP-MMP regions, we corrected for multiple comparisons using the Benjamini-Hochberg procedure to control the false discovery rate (FDR), that is, the expected proportion of type I errors (Benjamini and Hochberg, 1995). We then created 3D cortical surface visualizations showing the resulting FDR *q*-values across the HCP-MMP regions.

Subsequent to our primary analysis, we also examined the relationship between microstructure and demographic and behavioral measures. Besides demographic variables, we also analyzed measures of memory performance, negative intrusive thinking, and paternal substance abuse, which are factors related to THC exposure that we identified empirically from a preliminary analysis of the data. Our goal was then to assess their connection with both THC and gray matter microstructure. We estimated a multiple linear regression model relating microstructure variation to the combination of these measures. To reduce the complexity of the analysis, we summarized the microstructure parameters from FIC, AAIC, vmPFC, and the amygdala with a single general factor, by performing principal component analysis and extracting the scores of the first component. This general factor was used as a dependent variable in the regression model that included THC exposure, age, gender, BMI, smoking, drinking, memory, negative intrusive thinking, and paternal substance abuse as covariates.

Finally, we compared THC exposure as assessed from the urine screen with the self-reported total cannabis usage. We estimated linear regression models to test both the agreement of self-reported usage with THC test results and the association of self-reported results with microstructure parameters identified

**Table 1** Significant statistical associations between THC exposure and ODI

Region	$\Delta\text{BIC}$	$R^2$	$R_{\text{adj}}^2$	$\Delta R_{\text{adj}}^2$	std. $\beta$	SE	P-value
Frontoinsula	11.0	0.073	0.069	0.020	0.501	(0.119)	$2.9 \times 10^{-5}$
Anterior insular	8.0	0.111	0.106	0.016	0.443	(0.116)	$1.4 \times 10^{-4}$
Ventromedial PFC	5.7	0.106	0.100	0.014	0.409	(0.116)	$4.6 \times 10^{-4}$
Amygdala BLN-La	7.4	0.062	0.057	0.016	0.447	(0.119)	$1.8 \times 10^{-4}$
Amygdala INA	2.7	0.043	0.038	0.010	0.362	(0.119)	$2.3 \times 10^{-3}$
Amygdala ATA-ASTA	-0.9	0.073	0.068	0.006	0.280	(0.117)	$1.7 \times 10^{-2}$
General factor	18.0	0.124	0.119	0.027	0.573	(0.115)	$7.7 \times 10^{-7}$

Each row shows THC effects from a multiple linear regression model that included age, sex, BMI, intracranial volume, smoking and drinking as covariates. Data were centered and scaled to zero-mean and unit variance before modeling to standardize  $\beta$  coefficients. For each parameter, models were fit with and without THC exposure (as measured from a urine drug screen), and the change in BIC and  $R_{\text{adj}}^2$  was computed to further quantify the contribution of THC to the model. The results show the strongest effects were in fronto-insular cortex (FIC, AAIC) and the lateral portion of the basolateral amygdala (BLN-La). All results were from left-right averaged parameters. Other statistical results can be found in the supplementary material.

in the previous analysis. This was included to both confirm the validity of the THC test and to characterize dose-dependent effects, which are not otherwise available from the THC screen.

Our statistical analysis was implemented using R 3.3.3, plots were created using ggplot 3.2.1 (Wickham, 2017), and tables were created using stargazer 5.2.2 (Hlavac, 2013). Three-dimensional visualizations of statistical maps overlaid on brain anatomy were created using QIT.

## Results

Our primary analysis showed significant and strong associations between THC exposure and NODDI ODI in frontoinsula cortex (std.  $\beta = 0.501$ ,  $P = 2.9 \times 10^{-5}$ ) and three amygdala subfields comprising the lateral portion: the lateral basolateral nucleus (BLN-La) (std.  $\beta = 0.447$ ,  $P = 1.8 \times 10^{-4}$ ), the combined amygdala and amygdalostratial transition areas (ATA-ASTA) (std.  $\beta = 0.280$ ,  $P = 1.7 \times 10^{-3}$ ), and the intercalated nucleus (INA) (std.  $\beta = 0.362$ ,  $P = 2.3 \times 10^{-3}$ ). The data are shown in Figure 3A and B and regression results are summarized in Table 1. The statistical results are visualized on 3D models of the amygdala subfields in Figure 2B. No significant associations were found with other subcortical nuclei or with NODDI NDI. DTI FA showed similar effects as NODDI ODI, though with smaller effect sizes and larger P-values.

In our surface-based analysis of the cerebral cortex, we found significant associations between THC exposure and NODDI ODI in AAIC, several regions of comprising ventromedial cortex (Brodmann areas p32, s32, a24, and 10r), and several others weaker effects shown in Figure 2A. DTI FA showed similar results but with smaller effect sizes, and they can be found in the supplementary material. No significant associations were found with NODDI NDI. Because they exhibited bilateral symmetry, we focused on effects in agranular anterior insular and ventromedial prefrontal cortices, as illustrated in Figure 2A. Statistical analysis of the interhemispheric averages showed the strongest in frontoinsula cortex (std.  $\beta = 0.501$ ,  $P = 2.9 \times 10^{-5}$ ), vmPFC (std.  $\beta = 0.409$ ,  $P = 4.6 \times 10^{-4}$ ), and BLN-La of the amygdala (std.  $\beta = 0.447$ ,  $P = 1.8 \times 10^{-4}$ ). The AAIC overlapped substantially with the manually drawn FIC mask, but the effect sizes in AAIC were smaller than the those from FIC. The composite vmPFC region showed a stronger effect than the individual regions that comprised it, and the general factor showed the greater effect overall (std.  $\beta = 0.573$ ,  $P = 7.7 \times 10^{-7}$ ). The data are shown in Figure 3A and regression results are summarized in Table 1.

Regarding the model evaluation, FIC showed the strongest support for including THC exposure in the model ( $\Delta\text{BIC} = 11.0$ ),

and at the other extreme, the BIC suggested that in ATA-ASTA, the inclusion of THC exposure did not improve the model ( $\Delta\text{BIC} < 0$ ). The other areas showed positive (INA, vmPFC) to strong (AAIC, BLN-La) support for THC exposure improving the model (Kass and Raftery, 1995). In comparing the models from different diffusion parameters, the  $R^2$  coefficients of NODDI ODI models were generally higher than those from DTI FA.

Our analysis of behavioral parameters showed significant associations of the microstructure general factor score with: gender ( $\beta = 0.574$ ,  $P = 2.8 \times 10^{-4}$ ), BMI (std.  $\beta = 0.057$ ,  $P = 0.014$ ), memory (std.  $\beta = -0.102$ ,  $P = 0.042$ ), paternal substance abuse ( $\beta = 0.214$ ,  $P = 0.028$ ), and negative intrusive thinking (std.  $\beta = 0.137$ ,  $P = 7.8 \times 10^{-5}$ ). Furthermore, the effect of THC exposure retained significance and a large effect size when included with these covariates (std.  $\beta = 0.417$ ,  $P = 2.8 \times 10^{-4}$ ), and the total variance explained by the model was  $R^2 = 0.181$ . The data are shown in Figure 4 and the regression results are summarized in Table 2.

The comparison of self-reported cannabis use with the THC urine screen showed a strong correlation, indicating a substantial agreement between the two measures. Figure 3C shows plots of how the self-reported cannabis use scores relate to observed microstructure parameters. Multiple linear regression models showed similar significant associations as the urine screen; however, the models with self-reported cannabis use had smaller effect sizes and larger P-values than those from the urine screen. The largest individual effects with self-reported cannabis use were in FIC (std.  $\beta = 0.093$ ,  $P = 9.1 \times 10^{-6}$ ) and amygdala BLN-La (std.  $\beta = 0.103$ ,  $P = 1.07 \times 10^{-6}$ ), and the general factor showed the strongest effect overall (std.  $\beta = 0.122$ ,  $P = 5.86 \times 10^{-9}$ ). Figure 3C shows plots of how the self-reported cannabis usage scores relate to observed microstructure parameters, and the non-parametric local regression plot indicates the change in ODI is principally at the high end of the scale, where total reported uses exceeds 1000 uses.

A comprehensive summary of our experiments and results can be found in the supplementary material.

## Discussion

The present study combined high-quality multimodal neuroimaging data with advanced computational modeling approaches to characterize microstructure of the cerebral cortex and subcortical nuclei and how it relates to THC exposure. By analyzing the large cohort provided by the HCP, we quantitatively characterized microstructure variation in

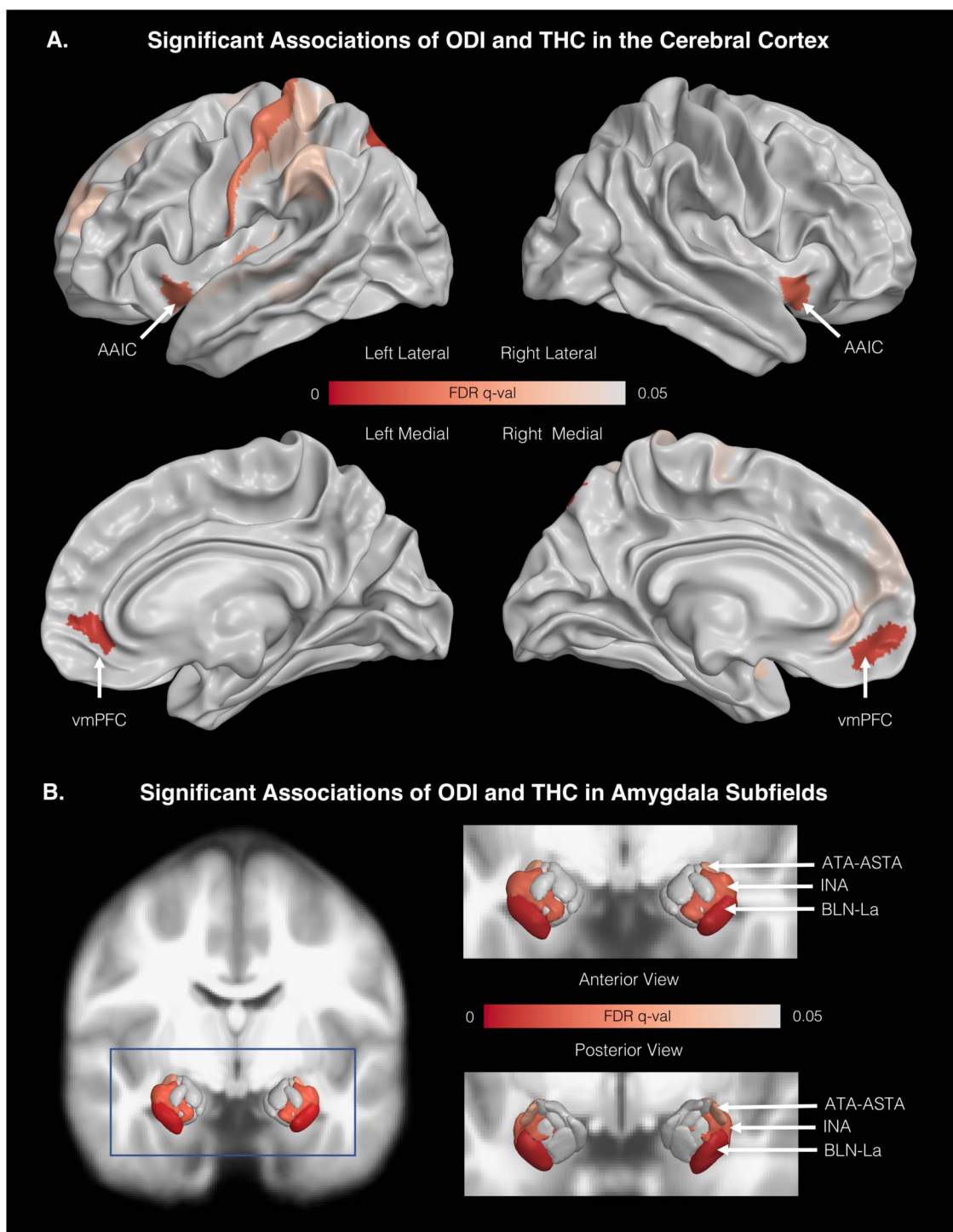


**Figure 2.** Visualizations showing anatomical areas with significant statistical associations between the ODI and THC exposure. (A) shows results from the cortical surface analysis, where there were strong bilateral effects in AAIC and ventromedial prefrontal cortex (vmPFC). (B) shows results from the amygdala subfield analysis, where three areas comprising the lateral portion were identified.

relation to biospecimen-defined THC exposure as it occurs in a typical non-clinical population. In particular, our analysis demonstrated that THC exposure is strongly associated with differential microstructure organization in the cerebral cortex and amygdala, and furthermore, that they are linked with independent effects in behavioral measures of memory per-

formance, negative intrusive thinking, and paternal substance abuse. Using computational anatomical modeling, our analysis enabled the localization of these effects in fronto-insular cortex, ventromedial prefrontal cortex, and lateral subfields of the amygdala. A comparison of diffusion parameters showed that the ODI had greater sensitivity to these effects, while DTI

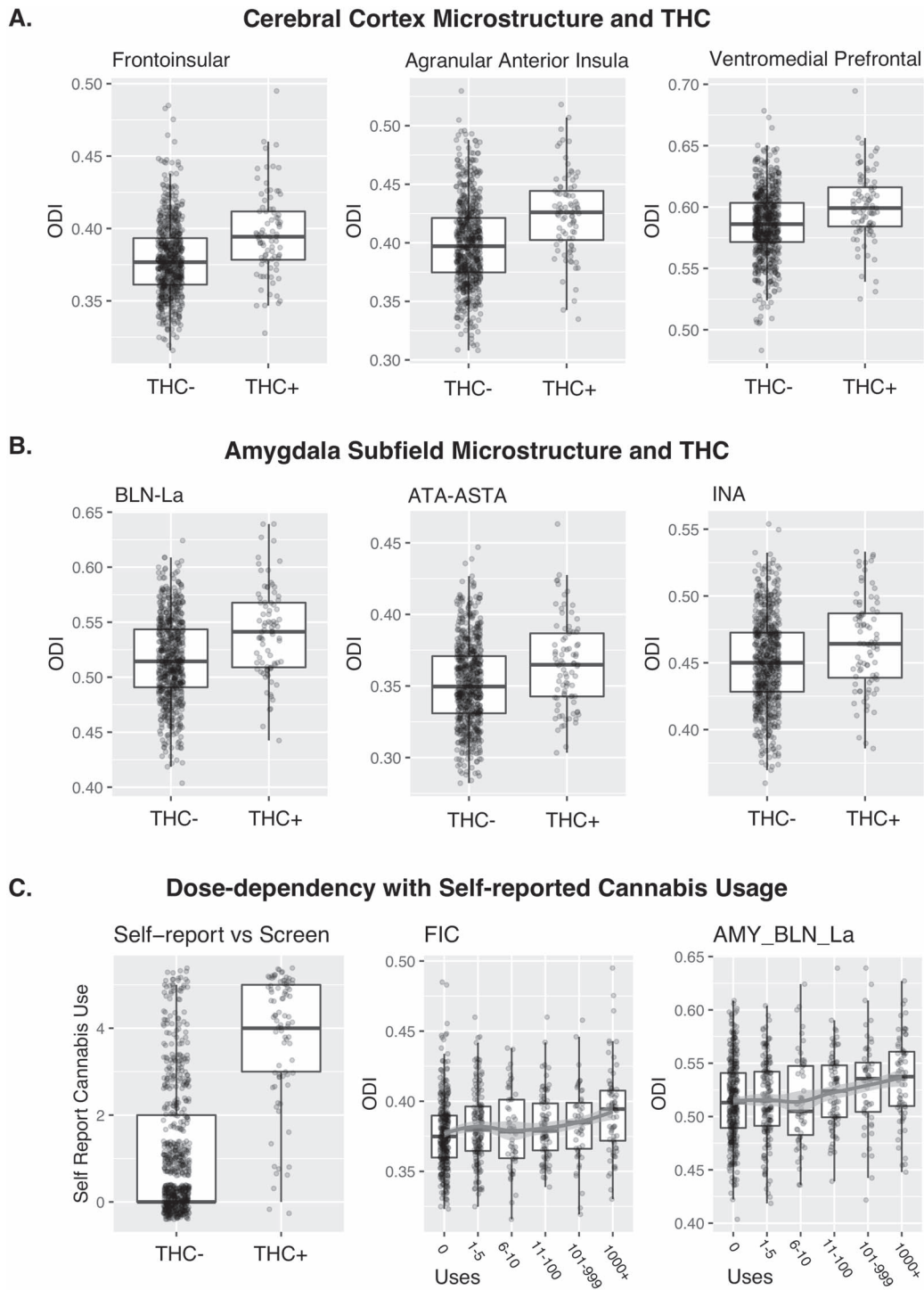
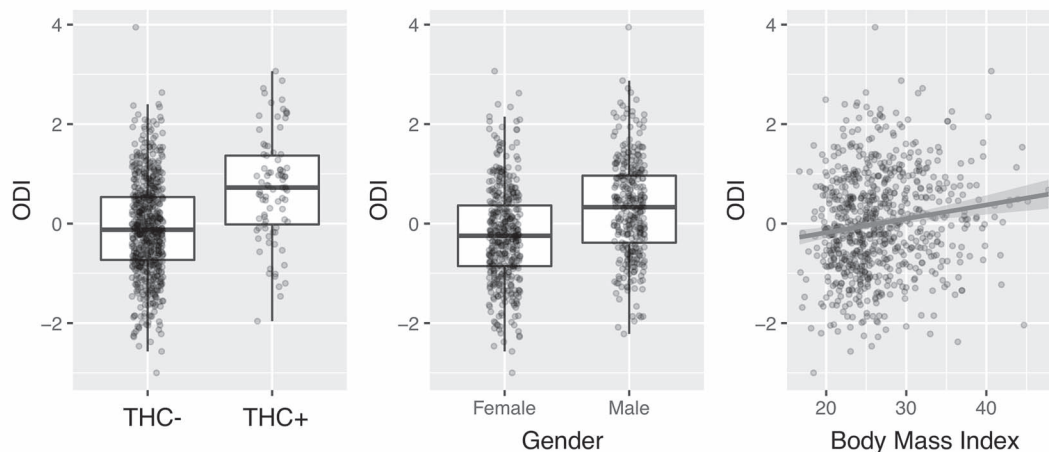


**Figure 3.** Plots showing the relationship between the ODI and THC exposure. (A) and (B) show associations between ODI and drug test results in cortical and amygdala gray matter. The results indicated THC exposure is associated with higher orientation dispersion. (C) shows analogous results with self-reported cannabis use. The first plot shows strong agreement between drug test results and self-reported use, and the second two plots show dose-dependency and ODI, wherein ODI has greater differences at the higher end of the scale. The plots include dots representing individual participants, and boxplots are overlaid to show the median and quartiles.

fractional isotropy detected them to a lesser extent. We focused on the urine drug screen as a primary indicator of THC exposure, and our statistical comparison of the drug test results with self-reported cannabis use suggested a close relationship. The results also provide some support for a dose-dependent effect,

as greater self-reported use was also associated with higher ODI. However, the THC urine screen proved the most sensitive for identifying brain associations with microstructure, perhaps because it affords a lower chance for reporting errors from participants. In addition, drug screens have been found to have

## A. A General Factor of Tissue Microstructure and Demographic Parameters



## B. A General Factor of Tissue Microstructure and Behavioral Characteristics

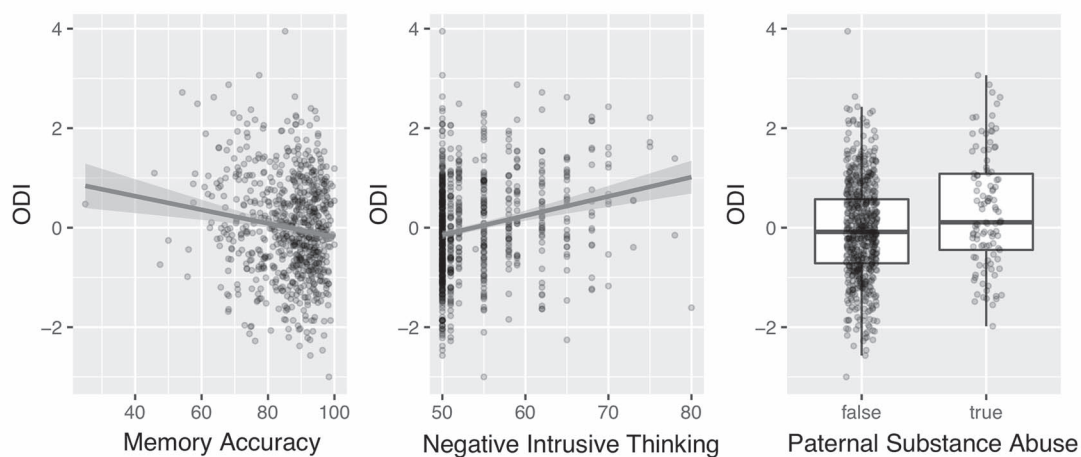


**Figure 4.** Plots showing the relationship between demographic and behavioral parameters and a general factor of ODI microstructure. The general factor was derived through principal component analysis of ODI values in FIC, AAC, VMPFC, BLN-La, ATA-ASTA, and INA. The top row shows the relationship between the ODI general factor and THC, gender, and BMI. ODI shows a positive trend with THC exposure, male subjects, and higher BMI. The second row shows the relationship between the ODI general factor and memory performance, negative intrusive thinking, and paternal substance abuse. The results indicate that poorer memory performance is associated with high ODI, as is a higher score on the thought problems scale and the paternal substance abuse. The plots include dots representing individual participants, and either boxplots or regression lines are overlaid to show the median and quartiles.

a dose-dependency of their own, in which heavy users have a longer time period in which they test positive (Moeller et al., 2017), a factor which may bias the THC positive participant pool toward those with higher levels of exposure. Furthermore, our results suggest that the observed effects are distinct from other substance use, including alcohol and nicotine.

Our findings support an emerging picture of the important link between fronto-insular cortex, prefrontal cortex and the amygdala and THC exposure, which is supported by past neuroimaging looking at CBF, functional activation, and morphometry with THC exposure. Several previous studies have specifically looked at brain changes with THC exposure in the HCP dataset, as we did in our study, and they found related changes in neuropsychological performance (Petker et al., 2019), poorer working memory with associated functional changes (Lorenzetti et al., 2019; Gilman et al., 2014; Owens et al., 2019), reduced amygdala and hippocampal volume (Pagliaccio et al., 2015;

Owens et al., 2019), reduced segregation between cognition and emotional function processing (Manza et al., 2019), and changes in white matter integrity (Orr et al., 2016). However, because no studies to date have yet explored the relationship between THC and gray matter microstructure, the present study represents a novel perspective on the structural organization of brain microanatomy in relation to THC. Specifically, we showed evidence that discrete brain areas are related to THC exposure, and furthermore, we found that the greatest sensitivity was obtained when deriving a single general factor from a linear combination of these areas. These findings raise several issues considering the endocannabinoid system and how exogenous THC exposure is perhaps related to measurable changes in tissue microstructure.

We can first consider our findings at a systems level, that is, related to functional aspects of fronto-insular cortex, ventromedial prefrontal cortex, and lateral amygdala. Our primary

**Table 2** Significant statistical associations between demographic and behavioral parameters and a general factor of ODI values ( $P < 0.05$ )

Variable	Std. $\beta$	SE	t-stat	P-value
THC positive	0.417	(0.115)	3.7	$2.8 \times 10^{-4}$
Gender	0.574	(0.088)	6.5	$9.9 \times 10^{-11}$
Age	0.057	(0.035)	1.7	0.10
Body Mass Index	0.021	(0.006)	3.2	<b>0.014</b>
Memory	-0.102	(0.035)	-2.9	<b>0.042</b>
Negative Intrusive Thinking	0.137	(0.035)	4.0	$7.8 \times 10^{-5}$
Paternal Substance Abuse	0.214	(0.097)	2.2	<b>0.028</b>
Daily Smoker	0.011	(0.015)	0.7	0.47
Daily Drinker	0.034	(0.019)	1.8	0.077
Intracranial Volume	-0.053	(0.044)	-1.2	0.22
Observations	768			
R <sup>2</sup>	0.181			
Adjusted R <sup>2</sup>	0.170			

The dependent variable was defined by the principal component scores computed to summarize NODDI ODI values in FIC, AAIC, vmPFC, BLN-La, ATA-ASTA and INA. Each row shows a different variable included in a single multiple linear regression model, and the columns list statistical parameters associated with them. The results show that gender, BMI, memory performance, paternal substance abuse, and negative intrusive thinking contribute to variation in the ODI general factor; however, with these covariates, THC retains a strong significant relationship with ODI indicating an independent contribution to variation in microstructure.

analysis aimed to understand microstructure variation in fronto-insular cortex, due to the comprehensive literature showing its role in salience processing (Seeley et al., 2007; Uddin, 2015; Menon and Uddin, 2010), interoceptive awareness (Craig, 2009), pain, decision making (Wiech et al., 2010), among many others (Nieuwenhuys, 2012). There is a plausible relationship between known effects of cannabis and our insular findings, for example, the representation of flavor in insular cortex (integration of taste and olfaction) (Small, 2010) and within the endocannabinoid system (Bellocchio et al., 2008); the processing of pain in anterior insula (Fazeli and Büchel, 2018; Wiech et al., 2010), and its commonality in gray matter morphometric studies of psychiatric illness (Goodkind et al., 2015). In addition to fronto-insular effects, the surface-based analysis showed the ventromedial prefrontal cortex as another discrete brain area where microstructure is related to THC exposure. Previous work has found that vmPFC serves a key role in emotional regulation (Hänsel and von Känel, 2008; Etkin et al., 2011), decision making (Bechara, Tranel, Damasio, 2000; Fellows and Farah, 2007; Reber et al., 2017), and psychopathology (Hiser and Koenigs, 2018; Myers-Schulz and Koenigs, 2012). Beyond the cortical effects, our analysis also showed anatomically specific effects within lateral amygdala subfields. Previous work studying the amygdala has shown its importance in emotion recognition (Adolphs, 2002) and social judgment (Adolphs et al., 1998). In conjunction with fronto-insular cortex, it is also involved in processing risk prediction error, uncertainty, and empathy (Singer et al., 2009; Decety and Michalska, 2010). Furthermore, Phan et al. (2008) showed related effects of THC on amygdala functional activity related to social signals, and our microstructure results show similar localization in lateral amygdala subfields.

We can draw several parallels among the functional significance of these brain areas. It is plausible that the observed effects exist because these areas work in concert; indeed, tract tracing studies of non-humans have shown direct connections among these three areas (Mufson et al., 1981; Amaral and Price, 1984), and functional studies have shown direct regulation of amygdala function by ventromedial prefrontal cortex (Motzkin et al., 2015; Coombs III et al., 2014) and perfusion changes linked to negative affect (Coombs III et al., 2014). Lesion studies have also shown its role coordinating the vmPFC and insular cortex

in risky decision making (Clark et al., 2008; Bechara, Tranel, Damasio, 2000), and our effects may further be linked to past work showing a connection between paternal alcohol abuse, and subsequent risky decision making and substance abuse in offspring (Ohannessian and Hesselbrock, 2008). With regard to our AAIC and vmPFC findings, the work of Baldo et al. suggest these areas play causal role in regulating feeding behavior via a GABA agonist, which possibly relates to the analogous role of THC on GABA inhibition. The areas identified in our study have also been proposed as a possible anatomical substrate for the somatic marker hypothesis, whereby the amygdala, insular and vmPFC process emotions to subsequently guide decision making (Bechara, Damasio, Damasio, 2000). A related point is that there were also parietal brain areas which showed moderate but significant effects (without bilaterality), including left hemisphere Brodmann areas 1, 7PL, and IP2, areas which all relate to somatosensory function. Furthermore, the meta-analysis by Goodkind et al. (2015) showed that while anterior insular cortex plays a role in both psychotic and non-psychotic psychiatric illnesses, the vmPFC exhibits specificity to psychotic cases, which is perhaps relevant to previously established associations between cannabis use and psychosis. In a direct comparison with their data, we found that our FIC and vmPFC regions have some overlap with those from the meta-analysis. In addition, given the pharmacological effects of THC on pain and the importance of fronto-insular cortex in the processing of pain expectation and prediction errors (Fazeli and Büchel, 2018; Craig, 2003; Hester et al., 2009), this supports the role of the endocannabinoid system in the processing of pain. Taking a broader view, our results suggest discrete brain areas in which the cannabinoid system may play its role in homeostatic regulation in which, as suggested by Volkow et al. (2017), it acts as a buffer against extreme experiences to promote well-being through its involvement in salience processing, emotion regulation, and decision making.

We can also drill further down to ask: what are plausible underlying cellular and molecular mechanisms that could produce these effects? One possibility is that our observations reflect a change in microglia density or activation, as Yi et al. (2019) rigorously showed that ODI parametrically reflects microglia density. This possibility is supported by work directly

showing changes in microglia in response to THC exposure (McHugh et al., 2014) and work showing that endocannabinoids are involved in microglia signaling (Stella, 2009) and driving them from quiescent to activated states (Mecha et al., 2015). The coordination of microglia and endocannabinoids have further been suggested to be a component of psychiatric disorders (Lisboa et al., 2016; Mecha et al., 2016), which is supported by our findings related to negative intrusive thinking (Abdellaoui et al., 2012). However, because microglia are found throughout the brain, this does not adequately explain the anatomical specificity of our findings.

To account for this, we propose a more parsimonious molecular and cellular mechanism: that THC exposure produces microstructural changes via the degradation of stathmin-2 (STMN2) at the presynaptic CB1 receptors (CBR1) of cholecystokinin (CCK) basket cells. STMN2 is a protein involved in the structural maintenance and repair of axons in adults (Klim et al., 2019), and THC has been shown to cause STMN2 degradation in growing axons in fetal brains thus disrupting connectivity (Tortoriello et al., 2014). The proposed role of STMN2 is driven in part due to the anatomical distribution of our findings, which showed a notable absence of effects in some cannabinoid-receptor-rich nuclei, i.e., caudate and putamen. We consulted the Genotype-Tissue Expression (GTEx) Portal (<https://gtexportal.org/>) and the Allen Brain Map Portal (<https://portal.brain-map.org/>) to observe expression profiles of the cannabinoid receptor protein CNR1, which showed widespread expression across the brain, including all of the investigated brain areas; however the distribution STMN2 and CCK provide interesting constraints. In contrast to CNR1, STMN2 showed negligible expression in the caudate, putamen, and substantia nigra but substantial expression in the cortex and amygdala. Concerning the cellular component, CCK basket cells are common interneurons whose morphology and inhibitory action are influenced by cannabinoids (Trettel and Levine, 2003; Berghuis et al., 2007) potentially through the degradation of STMN2. They have been previously identified in prefrontal cortex (Eggan et al., 2010), amygdala (Rovira-Esteban et al., 2017), and hippocampus (Hartzell et al., 2018), and the GTEx and Allen maps of CCK indicate expression patterns analogous with our findings, that is, more in amygdala and cortex and much less in the hypothalamus, caudate, putamen, substantia nigra, and periaqueductal gray. While we did not observe microstructure effects in hippocampus, we did observe significant differences in total hippocampal volume, similar to Owens et al. (2019), so higher resolution imaging data may be necessary to detect microstructural changes in the thin layer that CCK cells occupy. Thus, the effects of THC on STMN2 in CCK basket cells provides a plausible candidate mechanism explaining microstructural changes that are observable with diffusion MRI and consistent with the brain areas identified in our analysis.

Finally, there are several relevant factors with greater specificity than may be measurable with MRI, yet are still worth discussing. For example, fronto-insular and area 24 of ventromedial prefrontal cortex contain a unique and morphologically distinct population of cells, known as von Economo Neurons (VENs) (Nimchinsky et al., 1999; Allman et al., 2010), and due to their large size and bipolar geometry (Watson et al., 2006), it is plausible that changes in the relative size or local density of VENs in FIC could be a relevant factor. Some previous work has shown that the diffusion signal reflects compartment sizes consistent with cell bodies and dendrites (Latour et al., 1994), and others have performed simulations suggesting the possibility of detect-

ing VENs with multi-shell diffusion MRI (Menon et al., 2019). A final consideration is changes in dendritic spines and receptor density, which likely occur in conjunction with possible mechanisms described above. Specifically, there is evidence from Njoo et al. that cannabinoid receptor agonists cause the shrinkage of dendritic spines in mature cortical neurons in rodents, by selectively causing the collapse of the actin cytoskeleton within the spine (Njoo et al., 2015). Related work has shown similar changes in rodent dendritic spine morphology in prelimbic cortex (Miller et al., 2019), and when combined in stress, THC reduced mushroom spines in the rodent amygdala and impaired fear extinction (Saravia et al., 2019), which is perhaps relevant to acute THC side effects of anxiety and paranoia in humans. These possibilities align with the PET imaging finding that THC exposure downregulates CB1 receptor density (Hirvonen et al., 2012); however, it is unlikely these changes are directly observable with MRI, due to their fine spatial scale.

There are also several limitations which constrain what we can conclude from the present study. First and foremost, it is important to note that the causal nature of any explanation here should be carefully considered. While it could be that THC is causing changes in microstructure, it is also possible that distinct microstructure variants exist prior to THC exposure but predispose one to cannabis use through their behavioral correlates, e.g., impaired inhibition or a coping mechanism. However, our examination of self-reported cannabis use provides some clues related to dose-dependency, in which differences increased non-linearly with higher usage. However, it should be noted that the initial age of exposure is an important factor not explored in our study, and because endocannabinoids play a key role in neurodevelopment (Hurd et al., 2019), it would be valuable to understand how gray matter microstructure parameters vary in relation to adolescent exposure. The cross-sectional nature of the HCP young adult data prohibits a conclusive answer in this regard, requiring substantial further work that involves close tracking of THC exposure across the lifespan or perhaps with an interventional study design. Furthermore, while we examined exposure here through a THC-specific urine screen, participants may have been co-exposed to other phytocannabinoids, depending on the method of self-administration.

Regarding neuroimaging, our image analysis examined diffusion MRI estimates of microstructure properties, an approach that is powerful but with notable challenges related to data interpretation. MRI parameters are essentially statistical summaries of what is a large section of tissue, relative to the physical scale of neurons and other cells. Diffusion modeling has been shown in previous evaluation work to be sensitive to a variety of neuronal scale tissue properties, such as fiber coherence, packing density, myelination, etc. (Beaulieu, 2002); however, there remain challenges regarding its specificity in isolating the effects of any one of these factors. We employed two diffusion modeling approaches in an attempt to depict more specific organizational properties: first, we found effects related to FA using DTI; second, we complemented this with NODDI, an approach that shows promise in isolating the effects of neurite dispersion (Mollink et al., 2017; Schilling et al., 2018). These parameters show an interesting connection in gray matter; similar to Fukutomi et al. (2018), we found a high negative correlation between FA and ODI (Pearson's  $r = -0.78$ ). Furthermore, our experiments showed that NODDI ODI afforded greater sensitivity than DTI FA, suggesting that the findings may be distinguishable from neurite density, myelination, etc. In nearly all cases, the effect size of ODI was greater

than tensor anisotropy, suggesting that NODDI may provide distinct anatomical information for mapping the effects of THC exposure in gray matter. Finally, subsequent work could explore cerebellar gray matter, as it strongly expresses CNR1; however, there are challenges associated with surface-based modeling of cerebellar cortex and the optimization of NODDI fixed parameters in this region that require further attention as well.

In conclusion, the present study demonstrated strong associations between THC exposure and the differential organization of microstructure in the cerebral cortex and amygdala in a large cohort of young adults. We identified fronto-insular cortex, ventromedial prefrontal cortex, and the lateral amygdala as brain areas with the greatest relative differences in microstructure and found connections of these brain areas to independent effects in behavioral measures of memory, negative intrusive thinking, and paternal substance abuse. Given the increased usage of cannabis in many parts of the world, it is important to have a more complete understanding of how THC affects the brain. Our study complements a rich literature of neuroimaging studies of THC usage, and we expand on these past findings by showing that brain areas for salience processing, emotion regulation, and decision making also exhibit microstructure differences. Such structural effects potentially raise concerns regarding the long-term effects of cannabis use, and further studies are warranted to characterize the longitudinal nature of the onset and persistence of these effects across the lifespan and to investigate the causal neurobiological factors connecting THC exposure to microstructure changes in the endocannabinoid system.

## Supplementary Material

Supplementary material is available at *Cerebral Cortex* online.

## Acknowledgements

This work was supported by National Institutes of Health (grant number P41EB015922). Data were provided [in part] by the Human Connectome Project, WU-Minn Consortium (Principal Investigators: David Van Essen and Kamil Ugurbil; 1U54MH091657) funded by the 16 NIH Institutes and Centers that support the NIH Blueprint for Neuroscience Research; and by the McDonnell Center for Systems Neuroscience at Washington University. *Conflict of Interest:* The authors have no conflict of interest to report.

## Funding

This work was supported by the National Institute of Biomedical Imaging and Bioengineering (NIBIB) of the National Institutes of Health under award number.

## References

- Abdellaoui A, de Moor, Geels LM, Van Beek, Willemsen G, Boomsma DI. 2012. Thought problems from adolescence to adulthood: measurement invariance and longitudinal heritability. *Behav Genet.* 42:19–29.
- Achenbach TM. 2009. *The Achenbach System of Empirically Based Assessment (ASEBA): Development, Findings, Theory, and Applications*. Burlington, VT: University of Vermont Research Center for Children, Youth, & Families.
- Adolphs R. 2002. Neural systems for recognizing emotion. *Curr Opin Neurobiol.* 12:169–177.
- Adolphs R, Tranel D, Damasio AR. 1998. The human amygdala in social judgment. *Nature.* 470:393.
- Agrawal A, Madden PA, Buchholz KK, Heath AC, Lynskey MT. 2014. Initial reactions to tobacco and cannabis smoking: a twin study. *Addiction.* 109:663–671.
- Allman JM, Tetreault NA, Hakeem AY, Manaye KF, Semendeferi K, Erwin JM, Park S, Goubert V, Hof PR. 2010. The von Economo neurons in fronto-insular and anterior cingulate cortex in great apes and humans. *Brain Struct Funct.* 214:495–517.
- Amaral DG, Price J. 1984. Amygdalo-cortical projections in the monkey (*Macaca fascicularis*). *J Comp Neurol.* 230:465–496.
- Andrade C. 2016. Cannabis and neuropsychiatry, 2: the longitudinal risk of psychosis as an adverse outcome. *J Clin Psychiatry.* 77:e739–e742.
- Andre CM, Hausman J, Guerriero G. 2016. Cannabis sativa: the plant of the thousand and one molecules. *Front Plant Sci.* 7:19.
- Andreae MH, Carter GM, Shaparin N, Suslov K, Ellis RJ, Ware MA, Abrams DI, Prasad H, Wilsey B, Indyk D et al. 2015. Inhaled cannabis for chronic neuropathic pain: a meta-analysis of individual patient data. *J Pain.* 16:1221–1232.
- Arnone D, Barrick T, Chengappa S, Mackay C, Clark C, Abou-Saleh MT. 2008. Corpus callosum damage in heavy marijuana use: preliminary evidence from diffusion tensor tractography and tract-based spatial statistics. *Neuroimage.* 41:1067–1074.
- Ashtari M, Cervellione K, Cottone J, Ardekani BA, Sevy S, Kumra S. Diffusion abnormalities in adolescents and young adults with a history of heavy cannabis use. *J Psychiatr Res.* 43:189–204.
- Avants BB, Epstein CL, Grossman M, Gee JC. 2008. Symmetric diffeomorphic image registration with cross-correlation: evaluating automated labeling of elderly and neurodegenerative brain. *Med Image Anal.* 12:26–41.
- Basser PJ, Jones DK. 2002. Diffusion-tensor MRI: theory, experimental design and data analysis—a technical review. *NMR Biomed.* 15:456–467.
- Batalla A, Bhattacharyya S, Yuecel M, Fusar-Poli P, Crippa JA, Nogue S, Torrens M, Pujol J, Farre M, Martin-Santos R. 2013. Structural and functional imaging studies in chronic cannabis users: a systematic review of adolescent and adult findings. *PLoS One.* 8:e55821.
- Battistella G, Fornari E, Thomas A, Mall J-F, Chtioui H, Appenzeller M, Annoni J-M, Favrat B, Maeder P, Giroud C. 2013. Weed or wheel! FMRI, behavioural, and toxicological investigations of how cannabis smoking affects skills necessary for driving. *PLoS One.* 8:e52545.
- Battistella G, Fornari E, Annoni J-M, Chtioui H, Dao K, Fabritius M, Favrat B, Mall J-F, Maeder P, Giroud C. 2014. Long-term effects of cannabis on brain structure. *Neuropsychopharmacology.* 39:2041.
- Beaulieu C. 2002. The basis of anisotropic water diffusion in the nervous system—a technical review. *NMR Biomed.* 15:435–455.
- Bechara A, Damasio H, Damasio AR. 2000. Emotion, decision making and the orbitofrontal cortex. *Cereb Cortex.* 10:295–307.
- Bechara A, Tranel D, Damasio H. 2000. Characterization of the decision-making deficit of patients with ventromedial prefrontal cortex lesions. *Brain.* 123:2189–2202.
- Becker MP, Collins PF, Lim KO, Muetzel R, Luciana M. 2015. Longitudinal changes in white matter microstructure after heavy cannabis use. *Dev Cogn Neurosci.* 16:23–35.

- Bellocchio L, Cervino C, Pasquali R, Pagotto U. 2008. The endocannabinoid system and energy metabolism. *J Neuroendocrinol.* 20:850–857.
- Benjamini Y, Hochberg Y. 1995. Controlling the false discovery rate: a practical and powerful approach to multiple testing. *J R Stat Soc B Methodol.* 57:289–300.
- Berghuis P, Rajnecik AM, Morozov YM, Ross RA, Mulder J, Urbán GM, Monory K, Marsicano G, Matteoli M, Canty A et al. 2007. Hardwiring the brain: endocannabinoids shape neuronal connectivity. *Science.* 316:1212–1216.
- Bhattacharyya S, Crippa JA, Allen P, Martin-Santos R, Borgwardt S, Fusar-Poli P, Rubia K, Kambeitz J, Ocarroll C, Seal ML et al. 2012. Induction of psychosis by  $\delta$ 9-tetrahydrocannabinol reflects modulation of prefrontal and striatal function during attentional salience processing. *Arch Gen Psychiatry.* 69:27–36.
- Bhattacharyya S, Falkenberg I, Martin-Santos R, Atakan Z, Crippa JA, Giampietro V, Brammer M, McGuire P. 2015. Cannabinoid modulation of functional connectivity within regions processing attentional salience. *Neuropsychopharmacology.* 40:1343.
- Bloomfield MA, Hindocha C, Green SF, Wall MB, Lees R, Petrilli K, Costello H, Ogunbiyi MO, Bossong MG, Freeman TP. 2019. The neuropsychopharmacology of cannabis: a review of human imaging studies. *Pharmacol Ther.* 195:132–161.
- Borgwardt S, Allen P, Bhattacharyya S, Crippa FPJ, Seal M, Fraccaro V, Atakan Z, Rubia MROCK, McGuire PK. 2009. S39–03 neurofunctional effects of cannabis on response inhibition. *Eur Psychiatry.* 24:S208.
- Broyd SJ, van Hell, Beale C, Yuecel M, Solowij N. 2016. Acute and chronic effects of cannabinoids on human cognition—a systematic review. *Biol Psychiatry.* 79:557–567.
- Cabeen R, Laidlaw D, Toga A. 2018. Quantitative Imaging Toolkit: Software for Interactive 3D Visualization, Data Exploration, and Computational Analysis of Neuroimaging Datasets. In: *Proceedings International Society for Magnetic Resonance in Medicine (ISMRM)*. Vol 2018, p. 2854.
- Cabeen R, Sepehrband F, Toga A. 2019. Rapid and Accurate NODDI Parameter Estimation with the Spherical Mean Technique. In: *Proc International Society for Magnetic Resonance in Medicine (ISMRM)*. Vol 2019, p. 3363.
- Churchwell JC, Lopez-Larson M, Yurgelun-Todd DA. 2010. Altered frontal cortical volume and decision making in adolescent cannabis users. *Front Psychol.* 1:225.
- Clark L, Bechara A, Damasio H, Aitken M, Sahakian B, Robbins T. 2008. Differential effects of insular and ventromedial prefrontal cortex lesions on risky decision-making. *Brain.* 131:1311–1322.
- Colizzi M, McGuire P, Giampietro V, Williams S, Brammer M, Bhattacharyya S. 2018. Previous cannabis exposure modulates the acute effects of delta-9-tetrahydrocannabinol on attentional salience and fear processing. *Exp Clin Psychopharmacol.* 26:582.
- Coombs G III, Loggia ML, Greve DN, Holt DJ. 2014. Amygdala perfusion is predicted by its functional connectivity with the ventromedial prefrontal cortex and negative affect. *PLoS One.* 9:e97466.
- Craig A. 2003. A new view of pain as a homeostatic emotion. *Trends Neurosci.* 26:303–307.
- Craig A. 2009. How do you feel—now? The anterior insula and human awareness. *Nat Rev Neurosci.* 10:59–70.
- Decety J, Michalska KJ. 2010. Neurodevelopmental changes in the circuits underlying empathy and sympathy from childhood to adulthood. *Dev Sci.* 13:886–899.
- Devane WA, Dysarz FR, Johnson MR, Melvin LS, Howlett AC. 1988. Determination and characterization of a cannabinoid receptor in rat brain. *Mol Pharmacol.* 34:605–613.
- Devane WA, Hanus L, Breuer A, Pertwee RG, Stevenson LA, Griffin G, Gibson D, Mandelbaum A, Etinger A, Mechoulam R. 1992. Isolation and structure of a brain constituent that binds to the cannabinoid receptor. *Science.* 258:1946–1949.
- Dinov I, Van Horn, Lozev K, Magsipoc R, Petrosyan P, Liu Z, MacKenzie-Graha A, Eggert P, Parker DS, Toga AW. 2009. Efficient, distributed and interactive neuroimaging data analysis using the Loni pipeline. *Front Neuroinform.* 3:22.
- Eggan SM, Melchitzky DS, Sesack SR, Fish KN, Lewis DA. 2010. Relationship of cannabinoid cb1 receptor and cholecystokinin immunoreactivity in monkey dorsolateral prefrontal cortex. *Neuroscience.* 169:1651–1661.
- ElSohly MA, Gul W, Wanas AS, Radwan MM. 2014. Synthetic cannabinoids: analysis and metabolites. *Life Sci.* 97:78–90.
- Etkin A, Egner T, Kalisch R. 2011. Emotional processing in anterior cingulate and medial prefrontal cortex. *Trends Cogn Sci.* 15:85–93.
- Fazeli S, Büchel C. 2018. Pain-related expectation and prediction error signals in the anterior insula are not related to aversiveness. *J Neurosci.* 38:6461–6474.
- Fellows LK, Farah MJ. 2007. The role of ventromedial prefrontal cortex in decision making: judgment under uncertainty or judgment per se? *Cereb Cortex.* 17:2669–2674.
- Fischl B. 2012. Freesurfer *NeuroImage.* 62:774–781.
- Freund TF, Katona I, Piomelli D. 2003. Role of endogenous cannabinoids in synaptic signaling. *Physiol Rev.* 83:1017–1066.
- Fukutomi H, Glasser MF, Zhang H, Autio JA, Coalson TS, Okada T, Togashi K, Van Essen, Hayashi T. 2018. Neurite imaging reveals microstructural variations in human cerebral cortical gray matter. *Neuroimage.* 182:488–499.
- Gilman JM, Kuster JK, Lee S, Lee M, Kim B, Makris N, van der Kouwe, Blood AJ, Breiter HC. Cannabis use is quantitatively associated with nucleus accumbens and amygdala abnormalities in young adult recreational users. *J Neurosci.* 34:5529–5538.
- Glass M, Faull R, Dragunow M. 1997. Cannabinoid receptors in the human brain: a detailed anatomical and quantitative autoradiographic study in the fetal, neonatal and adult human brain. *Neuroscience.* 77:299–318.
- Glasser MF, Sotiropoulos SN, Wilson JA, Coalson TS, Fischl B, Andersson JL, Xu J, Jbabdi S, Webster M, Polimeni JR et al. 2013. The minimal preprocessing pipelines for the Human Connectome Project. *Neuroimage.* 80:105–124.
- Glasser MF, Coalson TS, Robinson EC, Hacker CD, Harwell J, Yacoub E, Ugurbil K, Andersson J, Beckmann CF, Jenkinson M et al. 2016. A multi-modal parcellation of human cerebral cortex. *Nature.* 536:171.
- Gonzalez R. 2007. Acute and non-acute effects of cannabis on brain functioning and neuropsychological performance. *Neuropsychol Rev.* 17:347–361.
- Goodkind M, Eickhoff SB, Oathes DJ, Jiang Y, Chang A, Jones-Hagata LB, Ortega BN, Zaiko YV, Roach EL, Korgaonkar MS et al. 2015. Identification of a common neurobiological substrate for mental illness. *JAMA Psychiat.* 72(4):305–315.
- Green B, Kavanagh D, Young R. 2003. Being stoned: a review of self-reported cannabis effects. *Drug Alcohol Rev.* 22:453–460.
- Grotenhermen F. 2003. Pharmacokinetics and pharmacodynamics of cannabinoids. *Clin Pharmacokinet.* 42:327–360.
- Grotenhermen F, Müller-Vahl K. 2012. The therapeutic potential of cannabis and cannabinoids. *Dtsch Arztebl Int.* 109:495.

- Gruber SA, Silveri MM, Dahlgren M, Deborah Y. 2011. Why so impulsive? White matter alterations are associated with impulsivity in chronic marijuana smokers. *Exp Clin Psychopharmacol.* 19:231.
- Hall W. 2015. What has research over the past two decades revealed about the adverse health effects of recreational cannabis use? *Addiction.* 110:19–35.
- Hall W, Degenhardt L. 2009. Adverse health effects of non-medical cannabis use. *Lancet.* 374(9698):1383–1391.
- Haney M, Hill MN. 2018. Cannabis and cannabinoids: from synapse to society. *Neuropsychopharmacology.* 43:1.
- Hänsel A, von Känel. 2008. The ventro-medial prefrontal cortex: a major link between the autonomic nervous system, regulation of emotion, and stress reactivity? *BioPsychoSocial Med.* 2:21.
- Harding IH, Solowij N, Harrison BJ, Takagi M, Lorenzetti V, Lubman DI, Seal ML, Pantelis C, Yücel M. 2012. Functional connectivity in brain networks underlying cognitive control in chronic cannabis users. *Neuropsychopharmacology.* 37:1923.
- Hartzell AL, Martyniuk KM, Brigidi GS, Heinz DA, Djaja NA, Payne A, Bloodgood BL. 2018. Npas4 recruits cck basket cell synapses and enhances cannabinoid-sensitive inhibition in the mouse hippocampus. *Elife.* 7:e35927.
- Hasin DS. 2017. US epidemiology of cannabis use and associated problems. *Neuropsychopharmacology.* 43:195.
- Heitzeg MM, Cope LM, Martz ME, Hardee JE, Zucker RA. 2015. Brain activation to negative stimuli mediates a relationship between adolescent marijuana use and later emotional functioning. *Dev Cogn Neurosci.* 16:71–83.
- Herkenham M, Lynn AB, Little MD, Johnson MR, Melvin LS, De Costa, Rice KC. 1990. Cannabinoid receptor localization in brain. *Proc Natl Acad Sci.* 87:1932–1936.
- Hester R, Nestor L, Garavan H. 2009. Impaired error awareness and anterior cingulate cortex hypoactivity in chronic cannabis users. *Neuropsychopharmacology.* 34:2450.
- Hirvonen J, Goodwin R, Li C-T, Terry G, Zoghbi S, Morse C, Pike V, Volkow N, Huestis M, Innis R. 2012. Reversible and regionally selective downregulation of brain cannabinoid cb 1 receptors in chronic daily cannabis smokers. *Mol Psychiatry.* 17: 642.
- Hiser J, Koenigs M. 2018. The multifaceted role of the ventromedial prefrontal cortex in emotion, decision making, social cognition, and psychopathology. *Biol Psychiatry.* 83:638–647.
- Hlavac M. 2013. Stargazer: latex code and ascii text for well-formatted regression and summary statistics tables. <http://CRAN.R-project.org/package=stargazer> (last accessed 3 September 2019).
- Hoy AR, Koay CG, Kecskemeti SR, Alexander AL. 2014. Optimization of a free water elimination two-compartment model for diffusion tensor imaging. *Neuroimage.* 103:323–333.
- Hua T, Vemuri K, Pu M, Qu L, Han GW, Wu Y, Zhao S, Shui W, Li S, Korde A et al. 2016. Crystal structure of the human cannabinoid receptor cb1. *Cell.* 167:750–762.
- Hurd YL, Manzoni OJ, Pletnikov MV, Lee FS, Bhattacharyya S, Melis M. 2019. Cannabis and the developing brain: insights into its long-lasting effects. *J Neurosci.* 39:8250–8258.
- Jacobus J, Squeglia L, Infante M, Bava S, Sciences TS. 2013. White matter integrity pre- and post marijuana and alcohol initiation in adolescence. *Brain Sci.* doi: 10.3390/brainsci3010396.
- Jacobus J, Squeglia LM, Meruelo AD, Castro N, Brumback T, Giedd JN, Tapert SF. 2015. Cortical thickness in adolescent marijuana and alcohol users: a three-year prospective study from adolescence to young adulthood. *Dev Cogn Neurosci.* 16:101–109. doi: 10.1016/j.dcn.2015.04.006.
- Jenkinson M, Beckmann CF, Behrens TE, Woolrich MW, Smith SM. 2012. *FSL NeuroImage.* 62:782–790.
- Kass RE, Raftery AE. 1995. Bayes factors. *J Am Stat Assoc.* 90:773–795.
- Klim JR, Williams LA, Limone F, San Juan IG, Davis-Dusenbery BN, Mordes DA, Burberry A, Steinbaugh MJ, Gamage KK, Kirchner R et al. 2019. Als-implicated protein tdp-43 sustains levels of stmn2, a mediator of motor neuron growth and repair. *Nat Neurosci.* 22:167–179.
- Kreitzer AC, Regehr WG. 2002. Retrograde signaling by endocannabinoids. *Curr Opin Neurobiol.* 12:324–330.
- Large M, Sharma S, Compton MT, Slade T, Nielssen O. 2011. Cannabis use and earlier onset of psychosis: a systematic meta-analysis. *Arch Gen Psychiatry.* 68:555–561.
- Latour LL, Svoboda K, Mitra PP, Sotak CH. 1994. Time-dependent diffusion of water in a biological model system. *Proc Natl Acad Sci.* 91:1229–1233.
- Lisboa SF, Gomes FV, Guimaraes FS, Campos AC. 2016. Microglial cells as a link between cannabinoids and the immune hypothesis of psychiatric disorders. *Front Neurol.* 7:5.
- Lisdahl KM, Wright NE, Christopher M, Maple KE, Shollenbarger S. 2014. Considering cannabis: the effects of regular cannabis use on neurocognition in adolescents and young adults. *Curr Addict Rep.* 1:144–156.
- Long T, Wagner M, Demske D, Leipe C, Tarasov PE. 2017. Cannabis in Eurasia: origin of human use and bronze age transcontinental connections. *Veg Hist Archaeobotany.* 26:245–258.
- Lopez-Larson MP, Bogorodzki P, Rogowska J, McGlade E, King JB, Terry J, Yurgelun-Todd D. 2011. Altered prefrontal and insular cortical thickness in adolescent marijuana users. *Behav Brain Res.* 220:164–172.
- Lorenzetti V, Chye Y, Silva P, Solowij N, Roberts CA. 2019. Does regular cannabis use affect neuroanatomy? An updated systematic review and meta-analysis of structural neuroimaging studies. *Eur Arch Psychiatry Clin Neurosci.* 269:59–71.
- Mackie K, Stella N. 2006. Cannabinoid receptors and endocannabinoids: evidence for new players. *AAPS J.* 8:E298–E306.
- Manza P, Shokri-Kojori E, Volkow ND. 2020. Reduced segregation between cognitive and emotional processes in cannabis dependence. *Cereb Cortex.* 30:628–639.
- Marconi A, Di Forti, Lewis CM, Murray RM, Vassos E. 2016. Meta-analysis of the association between the level of cannabis use and risk of psychosis. *Schizophr Bull.* 42:1262–1269.
- Mathew RJ, Wilson WH, Coleman RE, Turkington TG, DeGrado TR. 1997. Marijuana intoxication and brain activation in marijuana smokers. *Life Sci.* 60:2075–2089.
- Mattes RD, Engelman K, Shaw LM, Elsohly MA. 1994. Cannabinoids and appetite stimulation. *Pharmacol Biochem Be.* 49: 187–195.
- McHugh D, Roskowski D, Xie S, Bradshaw HB. 2014.  $\delta$ 9-thc and n-arachidonoyl glycine regulate bv-2 microglial morphology and cytokine release plasticity: implications for signaling at gpr18. *Front Pharmacol.* 4:162.
- Mecha M, Feliú A, Carrillo-Salinas F, Rueda-Zubiaurre A, Ortega-Gutiérrez S, de Sola, Guaza C. 2015. Endocannabinoids drive the acquisition of an alternative phenotype in microglia. *Brain Behav Immun.* 49:233–245.
- Mecha M, Carrillo-Salinas F, Feliú A, Mestre L, Guaza C. 2016. Microglia activation states and cannabinoid system: therapeutic implications. *Pharmacol Ther.* 166:40–55.

- Medina K, Nagel B, Neuroimaging TS. 2010. Abnormal cerebellar morphometry in abstinent adolescent marijuana users. *Psychiatry Res: Neuroimaging*.
- Menon V, Uddin LQ. 2010. Saliency, switching, attention and control: a network model of insula function. *Brain Struct Funct*. 214:655–667.
- Menon V, Guillermo G, Pinski MA, Nguyen V-D, Li J-R, Cai W, Wassermann D. 2019. Quantitative modeling links in vivo microstructural and macrofunctional organization of human and macaque insular cortex, and predicts cognitive control abilities. *bioRxiv*. doi: [10.1101/662601](https://doi.org/10.1101/662601).
- Miller ML, Chadwick B, Dickstein DL, Purushothaman I, Egervari G, Rahman T, Tessereau C, Hof PR, Roussos P, Shen L et al. 2019. Adolescent exposure to  $\delta$  9-tetrahydrocannabinol alters the transcriptional trajectory and dendritic architecture of prefrontal pyramidal neurons. *Mol Psychiatry*. 24:588.
- Moeller KE, Kissack JC, Atayee RS, Lee KC. 2017. Clinical interpretation of urine drug tests: what clinicians need to know about urine drug screens. In: *Mayo Clinic Proceedings*. Vol 92. Amsterdam: Elsevier, pp. 774–796.
- Mollink J, Kleinnijenhuis M, van Walsum, Sotiropoulos SN, Cottaar M, Mirfin C, Heinrich MP, Jenkinson M, Pallebage-Gamarallage M, Ansoorge O et al. 2017. Evaluating fibre orientation dispersion in white matter: comparison of diffusion mri, histology and polarized light imaging. *Neuroimage*. 157:561–574.
- Moore TH, Zammit S, Anne L, Barnes TR, Jones PB, Burke M, Lewis G. 2007. Cannabis use and risk of psychotic or affective mental health outcomes: a systematic review. *Lancet*. 370:319–328.
- Motzkin JC, Philippi CL, Wolf RC, Baskaya MK, Koenigs M. 2015. Ventromedial prefrontal cortex is critical for the regulation of amygdala activity in humans. *Biol Psychiatry*. 77:276–284.
- Mufson E, Mesulam M-M, Pandya D. 1981. Insular interconnections with the amygdala in the rhesus monkey. *Neuroscience*. 6:1231–1248.
- Murray RM, Morrison PD, Henquet C, Forti M. 2007. Cannabis, the mind and society: the hash realities. *Nat Rev Neurosci*. 8:nm2253.
- Myers-Schulz B, Koenigs M. 2012. Functional anatomy of ventromedial prefrontal cortex: implications for mood and anxiety disorders. *Mol Psychiatry*. 17:132.
- National Academies of Sciences, Engineering, and Medicine and others. 2017. *The health effects of cannabis and cannabinoids: The current state of evidence and recommendations for research*. Washington, DC: National Academies Press.
- Nestor L, Hester R, Garavan H. 2010. Increased ventral striatal bold activity during non-drug reward anticipation in cannabis users. *Neuroimage*. 49:1133–1143.
- Nieuwenhuys R. 2012. The insular cortex: a review. In: *Progress in Brain Research*. Vol 195. Elsevier, pp. 123–163.
- Nimchinsky EA, Gilissen E, Allman JM, Perl DP, Erwin JM, Hof PR. 1999. A neuronal morphologic type unique to humans and great apes. *Proc Natl Acad Sci*. 96:5268–5273.
- Njoo C, Agarwal N, Lutz B, Kuner R. 2015. The cannabinoid receptor cb1 interacts with the wave1 complex and plays a role in actin dynamics and structural plasticity in neurons. *PLoS Biol*. 13:e1002286.
- Ohannessian CM, Hesselbrock VM. 2008. Paternal alcoholism and youth substance abuse: the indirect effects of negative affect, conduct problems, and risk taking. *J Adolesc Health*. 42:198–200.
- Orr JM, Paschall CJ, Banich MT. 2016. Recreational marijuana use impacts white matter integrity and subcortical (but not cortical) morphometry. *NeuroImage: Clinical*. 12:47–56.
- Owens MM, MacKillop J, Sweet LH. 2019. Cannabis use is associated with lower hippocampus and amygdala volume: high-resolution segmentation of structural subfields in a large non-clinical sample. *PsyArXiv*. doi: <https://doi.org/10.31234/osf.io/3xytq>.
- Pagliaccio D, Barch DM, Bogdan R, Wood PK, Lynskey MT, Heath AC, Agrawal A. 2015. Shared predisposition in the association between cannabis use and subcortical brain structure. *JAMA Psychiat*. 72:994–1001.
- Pauli WM, Nili AN, Tyszkaj JM. 2018. A high-resolution probabilistic in vivo atlas of human subcortical brain nuclei. *Scientific data*. 5:180063.
- Petker T, Owens MM, Amlung MT, Oshri A, Sweet LH, MacKillop J. 2019. Cannabis involvement and neuropsychological performance: findings from the Human Connectome Project. *J Psychiatry Neurosci*. 44:1–9.
- Phan KL, Angstadt M, Golden J, Onyewuenyi I, Popovska A, de Wit. 2008. Cannabinoid modulation of amygdala reactivity to social signals of threat in humans. *J Neurosci*. 28:2313–2319.
- Quickfall J, Crockford D. 2006. Brain neuroimaging in cannabis use: a review. *J Neuropsychiatry Clin Neurosci*. 18:318–332.
- Reber J, Feinstein JS, Odoherly JP, Liljeholm M, Adolphs R, Tranel D. 2017. Selective impairment of goal-directed decision-making following lesions to the human ventromedial prefrontal cortex. *Brain*. 140:1743–1756.
- Rigucci S, Marques T, Forti DM, Taylor H, Mondelli D, Bonaccorso S, Simmons A, David A, Girardi P, Pariante C et al. 2015. Effect of high-potency cannabis on corpus callosum microstructure. *Psychol Med*. 46:841–854.
- Rovira-Esteban L, Péterfi Z, Vikór A, Máté Z, Szabó G, Hájos N. 2017. Morphological and physiological properties of cck/cb1r-expressing interneurons in the basal amygdala. *Brain Struct Funct*. 222:3543–3565.
- Saravia R, Ten-Blanco M, Julià-Hernández M, Gagliano H, Andero R, Armario A, Maldonado R, Berrendero F. 2019. Concomitant thc and stress adolescent exposure induces impaired fear extinction and related neurobiological changes in adulthood. *Neuropharmacology*. 144:345–357.
- Schilling KG, Janve V, Gao Y, Stepniewska I, Landman BA, Anderson AW. 2018. Histological validation of diffusion mri fiber orientation distributions and dispersion. *Neuroimage*. 165:200–221.
- Schnell T, Kleiman A, Euphrosyne G, Daumann J, Becker B. 2012. Increased gray matter density in patients with schizophrenia and cannabis use: a voxel-based morphometric study using DARTEL. *Schizophr Res*. 138:183–187.
- Schweinsburg AD, Schweinsburg BC, Medina KL, McQueeney T, Brown SA, Tapert SF. 2010. The influence of recency of use on fMRI response during spatial working memory in adolescent marijuana users. *J Psychoactive Drugs*. 42:401–412.
- Seeley WW, Menon V, Schatzberg AF, Keller J, Glover GH, Kenna H, Reiss AL, Greicius MD. 2007. Dissociable intrinsic connectivity networks for salience processing and executive control. *J Neurosci*. 27:2349–2356.
- Shollenbarger SG, Price J, Wieser J, Lisdahl K. 2015. Impact of cannabis use on prefrontal and parietal cortex gyrification and surface area in adolescents and emerging adults. *Dev Cogn Neurosci*. 16:46–53.

- Silvestri C, Di Marzo. 2013. The endocannabinoid system in energy homeostasis and the etiopathology of metabolic disorders. *Cell Metab.* 17:475–490.
- Singer T, Critchley HD, Preusschoff K. 2009. A common role of insula in feelings, empathy and uncertainty. *Trends Cogn Sci.* 13(8):334–340.
- Small DM. 2010. Taste representation in the human insula. *Brain Struct Funct.* 214:551–561.
- Smith LA, Azariah F, Lavender VT, Stoner NS, Bettiol S. 2015. Cannabinoids for nausea and vomiting in adults with cancer receiving chemotherapy. *Cochrane Database Syst Rev.* (11):CD009464.
- Sotiropoulos SN, Jbabdi S, Xu J, Andersson JL, Moeller S, Auerbach EJ, Glasser MF, Hernandez M, Sapiro G, Jenkinson M et al. 2013. Advances in diffusion MRI acquisition and processing in the Human Connectome Project. *Neuroimage.* 80:125–143.
- Stella N. 2009. Endocannabinoid signaling in microglial cells. *Neuropharmacology.* 56:244–253.
- Tarragon E, Moreno JJ. 2017. Role of endocannabinoids on sweet taste perception, food preference, and obesity-related disorders. *Chem Senses.* 43:3–16.
- Tortoriello G, Morris CV, Alpar A, Fuzik J, Shirran SL, Calvigioni D, Keimpema E, Botting CH, Reinecke K, Herdegen T et al. 2014. Miswiring the brain:  $\delta$ 9-tetrahydrocannabinol disrupts cortical development by inducing an scg10/stathmin-2 degradation pathway. *EMBO J.* 33:668–685.
- Trettel J, Levine ES. 2003. Endocannabinoids mediate rapid retrograde signaling at interneuronâ€™ pyramidal neuron synapses of the neocortex. *J Neurophysiol.* 89:2334–2338.
- Tyszka JM, Pauli WM. 2016. In vivo delineation of subdivisions of the human amygdaloid complex in a high-resolution group template. *Hum Brain Mapp.* 37:3979–3998.
- Uddin LQ. 2015. Salience processing and insular cortical function and dysfunction. *Nat Rev Neurosci.* 16:55.
- Van Essen, Smith SM, Barch DM, Behrens TE, Yacoub E, Ugurbil K, Consortium W-MH et al. 2013. The WU-Minn Human Connectome Project: an overview. *Neuroimage.* 80:62–79.
- van Hell, Bossong MG, Jager G, Kristo G, van Osch, Zelaya F, Kahn RS, Ramsey NF. 2011. Evidence for involvement of the insula in the psychotropic effects of thc in humans: a double-blind, randomized pharmacological mri study. *Int J Neuropsychopharmacol.* 14:1377–1388.
- Volkow ND, Baler RD, Compton WM, Weiss SR. 2014. Adverse health effects of marijuana use. *N Engl J Med.* 370:2219–2227.
- Volkow ND, Hampson AJ, Baler RD. 2017. Don't worry, be happy: endocannabinoids and cannabis at the intersection of stress and reward. *Annu Rev Pharmacol Toxicol.* 57:285–308.
- Vrieze SI. 2012. Model selection and psychological theory: a discussion of the differences between the akaike information criterion (aic) and the bayesian information criterion (bic). *Psychol Methods.* 17:228.
- Watson KK, Jones TK, Allman JM. 2006. Dendritic architecture of the von Economo neurons. *Neuroscience.* 141:1107–1112.
- Wetherill RR, Fang Z, Jagannathan K, Childress A, Rao H, Franklin TR. 2015. Cannabis, cigarettes, and their co-occurring use: disentangling differences in default mode network functional connectivity. *Drug Alcohol Depend.* 153:116–123.
- Whiting PF, Wolff RF, Deshpande S, Di Nisio, Duffy S, Hernandez AV, Keurentjes JC, Lang S, Misso K, Ryder S et al. 2015. Cannabinoids for medical use: a systematic review and meta-analysis. *JAMA.* 313:2456–2473.
- Wickham H. 2017. The tidyverse. R package ver. 1:1.
- Wiech K, Lin C-s, Brodersen KH, Bingel U, Ploner M, Tracey I. 2010. Anterior insula integrates information about salience into perceptual decisions about pain. *J Neurosci.* 30:16324–16331.
- Yi SY, Barnett BR, Torres-Velázquez M, Zhang Y, Hurley SA, Rowley PA, Hernando D, Yu J-PJ. 2019. Detecting microglial density with quantitative multi-compartment diffusion mri. *Front Neurosci.* 13:81.
- Yücel M, Zalesky A, Takagi MJ, Bora E, Fornito A, Ditchfield M, Egan GF, Pantelis C, Lubman DI. 2010. White-matter abnormalities in adolescents with long-term inhalant and cannabis use: a diffusion magnetic resonance imaging study. *J Psychiatry Neurosci.* 35:409–412.
- Zalesky A, Solowij N, Yücel M, Lubman DI, Takagi M, Harding IH, Lorenzetti V, Wang R, Searle K, Pantelis C et al. 2012. Effect of long-term cannabis use on axonal fibre connectivity. *Brain.* 135:2245–2255.
- Zhang H, Yushkevich PA, Alexander DC, Gee JC. 2006. Deformable registration of diffusion tensor mr images with explicit orientation optimization. *Med Image Anal.* 10:764–785.
- Zhang H, Avants BB, Yushkevich PA, Woo JH, Wang S, McCluskey LF, Elman LB, Melhem ER, Gee JC. 2007. High-dimensional spatial normalization of diffusion tensor images improves the detection of white matter differences: an example study using amyotrophic lateral sclerosis. *IEEE Trans Med Imaging.* 26:1585–1597.
- Zhang H, Schneider T, Wheeler-Kingshott CA, Alexander DC. 2012. Noddi: practical in vivo neurite orientation dispersion and density imaging of the human brain. *Neuroimage.* 61:1000–1016.
- Zhang S, Peng H, Dawe RJ, Arfanakis K. 2011. Enhanced ICBM diffusion tensor template of the human brain. *Neuroimage.* 54:974–984.